

Congestion Risk-Aware Unit Commitment With Significant Wind Power Generation

Sajjad Abedi [✉], Member, IEEE, Miao He, Senior Member, IEEE, and Diran Obadina, Senior Member, IEEE

Abstract—Large-scale and ubiquitous penetration of wind power generation to power systems necessitates more conservative provision of system reliability by ensuring adequately committed reserve and observance of transmission constraints. In addition, wind power curtailment due to the technical limitations of system operations, such as transmission congestion, should be efficiently mitigated. To this aim, this paper presents a congestion risk-aware unit commitment formulation in a two-settlement market environment. The uncertainty impact of multicorrelated wind power and contingencies on the risk of transmission congestion for each line, called the *Line Transfer Margins* (LTM), is incorporated using basic statistical data on the nodal wind power forecast and probability of credible line-outages across the system. The LTMs, formulated free of any distributional assumptions, collectively provide a measure for transmission reserves, which effectively mitigate the likelihood of transmission congestion, reserve undeliverability, and wind power curtailment in the real-time economic dispatch. The effectiveness of the proposed approach is verified through comparative case studies on IEEE RTS-96 for various wind power and LTM scenarios.

Index Terms—Congestion management, line transfer margin, unit commitment, wind power uncertainty, power system reliability, wind power curtailment, transmission reserve.

NOMENCLATURE

A. Parameters

c	Generation cost coefficient [\$/h]
sc	Start-up cost coefficient [\\$]
nc	No-load cost coefficient [\\$]
rc	Reserve cost coefficient [\$/h]
B	DC power flow bus susceptance matrix [p.u.]
n_T	No. of time slots in real-time dispatch horizon
P_{\max}	Branch capacity rating [p.u.]
p_{\max}^{\max}	Generator's maximum output level [p.u.]
p_{\min}^{\min}	Generator's minimum output level [p.u.]
d	Nodal demand power [p.u.]
\hat{w}	Wind farm output forecast in day-ahead UC [p.u.]

Manuscript received November 9, 2017; revised February 28, 2018; accepted April 22, 2018. Date of publication April 30, 2018; date of current version October 18, 2018. This work was supported in part by Electric Reliability Council of Texas (ERCOT), and in part by the National Science Foundation (NSF) under Grant ECCS-1509890 and ECCS-1653922. (Corresponding author: Sajjad Abedi.)

S. Abedi and M. He are with the Department of Electrical and Computer Engineering, Texas Tech University, Lubbock, TX 79409 USA (e-mail: S.Abedi@ttu.edu; Miao.He@ttu.edu).

D. Obadina is with the Electric Reliability Council of Texas, Taylor, TX 76574 USA (e-mail: Diran.Obadina@ercot.com).

Color versions of one or more of the figures in this paper are available online at <http://ieeexplore.ieee.org>.

Digital Object Identifier 10.1109/TPWRS.2018.2831677

P_{ex}	Probability of exceedance in point forecast method
ζ	Power Transfer Distribution Factor (PTDF)
R	Matrix of spatial correlation among wind generators
α	Conservativeness factor for line transfer margins
γ	Reserve capacity coefficient
R^{10}	10-min ramp rate [p.u./h]
R^U, R^D	Ramp up/down rate [p.u./h]
UT, DT	Generator's minimum up/down time [h]
W	Penalty weight coefficient

B. Indices and Sets

\mathcal{G}	Set of conventional generation units, $g \in \mathcal{G}$
\mathcal{L}	Set of transmission lines, $l \in \mathcal{L}$
\mathcal{N}	Set of buses (nodes), $n \in \mathcal{N}$
\mathcal{T}	Time length of scheduling horizon, $t \in \mathcal{T}$
\mathcal{R}	Real-time dispatch time slot index, $\rho_0 \in \mathcal{R}$

C. Variables

sd, su	Shut-down/Start-up binary variable
u	Unit on/off binary variable
w	Wind farm output random variable [p.u.]
w_{rt}	Wind power realization in real-time dispatch [p.u.]
w_{cr}	Curtailed wind power in real-time dispatch [p.u.]
p_g	Generator's active power production [p.u.]
p_l	Line's active power flow [p.u.]
r_g	Generator's spinning reserve [p.u.]
Γ	Line Transfer Margin (LTM) [p.u.]
θ	Voltage angle difference across a line [rad]

I. INTRODUCTION

THE ever-increasing penetration of wind energy resources into power generation portfolio has led to several emerging challenges for electric utilities to overcome the imposed uncertainties in the operating plans and to provide reliable, efficient and economical system operations. The uncertain nature of wind energy results in large power flow fluctuations over a short period of time, making effective utilization of wind power a grand challenge especially in congestion-prone networks. Therefore, congestion management in transmission system is more pronounced in power systems with high wind energy penetration as new wind capacity deployments may introduce further unexpected bottlenecks in the grid. When generation reserve is undeliverable due to binding power flow constraints, utility operators may resort to either curtailment of a remarkable portion of wind energy, or shedding a portion of the load [1], [2]. Wind power curtailment thereby increases the operation costs, escalates

revenue uncertainty for wind power producers, and demoralizes future investments in the wind energy [3]. It can be observed that the reliability issues raised by integration of uncertain wind power are interrelated.

Several types of solutions have been devised to alleviate the consequences of wind power uncertainty on power system operations. The first group of solutions rely on infrastructural supplements for balancing the variability [4]–[11]. Specifically, employing demand response resources [4], deployment of energy storage systems (EES) [5], and use of Flexible AC Transmission Systems (FACTS) to control power flows and manage congestion [6] have been studied. The work presented in [5] studies a generation re-dispatch method considering the dynamic interactions among wind energy curtailment, generator ramp rates and EES, where the performance of the mitigation measure in terms of total energy curtailment, congestion costs, line load factor and congestion probability is assessed. The coordination of hydropower [8], pumped storage planning [10] and compressed air storage [11] with wind power in the day-ahead Unit Commitment (UC) is pursued in order to minimize wind energy curtailments during congestion situations. A fundamental drawback associated with these efforts is that they often presume sufficient availability of the supplemental resources (e.g. EES), without accounting for the required capital cost, long-term planning or other integration and operation issues of the equipment.

The second group of strategies has been directed towards improvements in the *flexibility* and *adaptability* in system operations to increase the capability of facing unexpected wind power realizations, while maintaining the minimum impact on the reliability of the grid as well as the capital and operational costs. In this paradigm, the findings primarily offer enhanced utilization of the existing network infrastructure, including generation and transmission system, without the need to expensive investment on network reinforcement, such as network expansion and development of EES. The operational decisions in the UC and economic dispatch (ED) problems are modified ahead or near the real-time operation such that the optimal dispatch is achieved and further robustness to wind power forecast error is assured. In [12], increasing demand responsiveness by using real-time retail price signals has been examined as a way to reducing the redispatch cost incurred by wind power forecast error. Improving accuracy of wind power forecasts [13], [14], adopting stochastic optimization techniques in the day-ahead UC and ED problems to cover a credible range of future wind power scenarios in the UC [15], [16], as well as methods towards characterizing adequate amount of reserve capacity and transfer capability [17], [18] lie in this group.

Another way of achieving operational flexibility is flexible utilization of transmission system for congestion management and mitigation of wind power curtailment, such as modifying network topology by transmission switching [19], [20], where moving from the infeasible or binding power flow conditions to feasible ones at the least cost is pursued in congestion redispatch. Another approach based on probabilistic constraints in Optimal Power Flow (OPF) is presented in [21], assuming a Gaussian distribution for wind power uncertainty.

Dynamic Line Rating (DLR) has been identified as a method to maximize the utilization of the available transmission capacity leading to better congestion prevention and improved wind power delivery [22]. In wind-rich regions, the DLR can attempt to increase thermal line capacity in the UC to accommodate increased wind farm output into the nearby network [23]. However, continuous weather monitoring and rating of the line capacities is required to avoid potential over-ratings.

In addition to the mere gain in thermal line capacity, the operational flexibility could be achieved by incorporating predictive models of the line flow uncertainty such that the scheduled reserve capacity can better alleviate congestion. Along this venue, this paper presents a systematic approach to reserve a portion of total transmission capacity accounting for the risk of wind power uncertainty-induced congestion. In summary, the contributions made in this work are listed as follows:

- The risk of line flow congestion induced by spatially-dispersed correlated wind power sources is systematically characterized by formulating LTM, which specifies an upper limit on congestion probability on each line in a *Risk-Aware* UC framework. The LTM could be easily pre-calculated using basic statistical and network information regardless of the type of distribution, specifically, the mean and variance of nodal wind power forecast distribution, as well as operational distribution factors, with no considerable increase in computational complexity for solving the UC problem. Moreover, the LTM can be easily extended to account for the line flow uncertainty caused by credible line outages. Further, performance of the proposed method is extensively analyzed by adopting real-time redispatch method where infeasible cases are identified to quantify congestion frequency function.
- By incorporating the risk of transmission congestion in form of LTMs, the resultant risk-aware UC formulation is formed as a deterministic optimization problem, which avoids the complexity induced by exponentially-growing scenarios in stochastic optimization approaches [24].

In this paper, a clear formulation and refined model of LTM is tuned, and sensitivity of LTM to key parameters is presented. Moreover, the initial study of this method in [25] is extended to a real-time redispatch framework to analyse the performance of the proposed method from various operational metrics, conducting detailed numerical analysis to assess operation cost, congestion likelihood, wind power curtailment, load shedding and available reserve capacity. The structure of this paper is as follows: In Section II, the formulation and sensitivity analysis of LTM is developed, and a deterministic risk-aware UC with LTM is presented. Section III discusses the ED formulation to evaluate the performance of the proposed method in real-time operation. Numerical results and discussion follows in Section IV. Finally, Section V concludes this paper.

II. PROBLEM FORMULATION

A. Quantifying Risk of Uncertainty-Induced Congestion

Due to the probabilistic nature of wind power forecast, line flows also appear stochastic in real-time dispatch. Hence, the

LTM is aimed at reflecting the impact of nodal wind power uncertainty on the capacity utilization of transmission lines. Using LTM imposes an upper bound to the probability of line congestion and assigns a margin on the transmission capacity to be capable of accommodating extreme wind power scenarios, especially when the forecast exhibits large error.

The nodal wind power forecast distribution can be simply represented by the probability density function (PDF) of nodal wind power w_n at bus n for each scheduling time step t characterized by its mean, $E[w_n^t] = \mu_{w_n^t}$, and variance, $\sigma_{w_n^t}^2$. The day-ahead point forecast of wind power is obtained by adopting the probability of exceedance (POE) given the Cumulative Distribution Function (CDF) of wind power forecast information for each time step, as follows:

$$\hat{w}_n^t = F_{w_n^t}^{-1}(1 - P_{ex}), n \in \mathcal{N} \quad (1)$$

The probability of congestion occurrence for each line is expressed by:

$$\pi(p_l \geq P_l^{\max}), l \in \mathcal{L} \quad (2)$$

The goal of derivation of LTM is to characterize the risk of congestion due to branch flows caused by wind power uncertainty. Therefore, the branch flows can be broken down to their components, as follows:

$$p_l = p_l^g - p_l^{nl} \quad (3)$$

where p_l^g and p_l^{nl} are the branch flow components from conventional generators and net load, respectively. The net load is $p_l^{nl} = p_l^{\text{load}} - p_l^w$, where p_l^{load} is the flow in line l from load demand and p_l^w is the flow in the same line from wind power sources.

The probability in Eq. (2) can be written as:

$$\begin{aligned} \pi(p_l \geq P_l^{\max}) &= \pi(p_l^g - p_l^{nl} \geq P_l^{\max}) \\ &= \pi(-p_l^{nl} \geq P_l^{\max} - p_l^g) = \pi(-p_l^{nl} \geq P_l'^{\max}) \\ &= \pi(-p_l^{nl} - E[-p_l^{nl}] \geq P_l'^{\max} - E[-p_l^{nl}]), \\ P_l'^{\max} &= P_l^{\max} - p_l^g \end{aligned} \quad (4)$$

where $E[-p_l^{nl}]$ is the mean value of power flow in line l at the current time step under all possible wind power scenarios as characterized by nodal wind power forecast distributions, and p_l is positive. $P_l'^{\max}$ is the maximum power flow capacity available for the wind power-induced flows in line l in the UC. For negative p_l , the equations are quite similar, where p_l could be replaced by $-p_l$. From the DC power flow analysis, p_l can be expressed in terms of Power Transfer Distribution Factor (PTDF) by the following equation:

$$p_l^{nl} = \sum_{n=1}^N \zeta_{n,l} \cdot (d_n - w_n), n \in \mathcal{N}, l \in \mathcal{L} \quad (5)$$

Since the PTDF links the line flows to the nodal power injections, the mean and variance values of p_l^{nl} is based upon the

distribution of nodal wind power forecast:

$$E[p_l^{nl}] = \sum_{n=1}^N \zeta_{n,l} \cdot (d_n - E[w_n]) \quad (6)$$

$$\sigma_{p_l^{nl}}^2 = \zeta_l \boldsymbol{\sigma}_w \mathbf{R}_w \boldsymbol{\sigma}_w \zeta_l^T \quad (7)$$

where \mathbf{R} and $\boldsymbol{\sigma}_w$ represent the correlation matrix and the diagonal standard deviation matrix of the output power forecast of the wind farms, respectively. The load forecast error is neglected compared to wind power forecast error. ζ_l is the PTDF matrix.

According to the Cantelli's inequality [26], an upper bound on the probability in (2) is given as:

$$\pi(-p_l^{nl} \geq P_l'^{\max}) \leq \pi_c^{\max} \quad (8)$$

where

$$\pi_c^{\max} = \frac{\sigma_{p_l^{nl}}^2}{\sigma_{p_l^{nl}}^2 + [P_l'^{\max} - E[-p_l^{nl}]]^2} \quad (9)$$

In order to maintain the required security limit based on the LTM model, the system operator can set the parameter α , called as "Conservativeness Factor", depending on the degree of conservativeness about assessing the probability of congestion, and the corresponding line capacity margin that can be occupied by wind power flow. In other words, the higher value assigned to α , the lower is the imposed probability bound of congestion with respect to π_c^{\max} and thus, a larger margin of wind power as a portion of line capacity is assigned as the risk margin characterized by LTM.

$$\pi_c^{\max} \leq \frac{1}{\alpha^2} \quad (10)$$

$$-E[p_l^{nl}] \leq P_l'^{\max} - \sigma_{p_l^{nl}} \sqrt{\alpha^2 - 1} \quad (11)$$

Using (10) and (11), the following expression is derived in form of transmission capacity constraint:

$$-p_l^{nl} \leq P_l'^{\max} - p_l^{nl} + E[p_l^{nl}] - \sigma_{p_l^{nl}} \sqrt{\alpha^2 - 1} \quad (12)$$

Eq. (12) can be rewritten as:

$$-p_l^{nl} \leq P_l'^{\max} + \sum_{n=1}^N \zeta_{n,l} \cdot (w_n - E[w_n]) - \sigma_{p_l^{nl}} \sqrt{\alpha^2 - 1} \quad (13)$$

By using (3), (13) and substituting for $P_l'^{\max}$ from (4), the new transmission capacity constraint in the UC is characterized as follows:

$$p_l \leq P_l^{\max} + \sum_{n=1}^N \zeta_{n,l} \cdot (w_n - E[w_n]) - \sigma_{p_l^{nl}} \sqrt{\alpha^2 - 1} \quad (14)$$

where $\sigma_{p_l} = \sigma_{p_l^{nl}}$. By adding the time index, the LTM for the line l at the time t can be introduced as follows:

$$\Gamma_l^t \triangleq - \sum_{n=1}^N \zeta_{n,l} \cdot (w_n^t - E[w_n^t]) + \sigma_{p_l}^t \sqrt{\alpha^2 - 1}, \quad (p_l \geq 0) \quad (15)$$

For the case of negative line flows, the LTM formulation remains exactly the same, as we can simply replace p_l by $-p_l$ in (3).

Therefore, the following equation can be used for negative lines flows:

$$\Gamma_l^t \triangleq \sum_{n=1}^N \zeta_{n,l} \cdot (w_n^t - E[w_n^t]) + \sigma_{p_l}^t \sqrt{\alpha^2 - 1}, \quad (p_l < 0) \quad (16)$$

By using LTM, a congestion risk-aware day-ahead generation and reserve commitment is achieved, which is capable of mitigating the likelihood of line congestions and redispatch cost in real-time operation caused by wind power forecast error. In the proposed LTM model, in addition to the PDF associated with nodal wind power forecast, the spatial correlations among the forecast distribution of different wind farms are considered. It is noteworthy that the proposed method is independent from the type of the probability distribution of the wind power forecast, as it only requires the mean and standard deviation of the data. This is the reason why there is no need to distribution assumptions in the formulation of LTM.

B. Impact of Contingency and Curtailment

LTM is defined to quantify a risk margin for transmission congestion, caused by wind power uncertainty. In order to efficiently manage possible congestions, other uncertainty sources for day-ahead schedules could also be considered, including credible $N - 1$ line-outage contingencies and possible wind power curtailment. These factors can be characterized in the LTM model, as follows.

Let $\beta_{k,l}$ denote the Line Outage Distribution Factor (LODF) of line flow l to the $N - 1$ contingency at line (k, l) . Then, by borrowing the method in reference [27], line flow p_l by taking into account $N - 1$ line-outage contingencies is given by:

$$p_l = \sum_{n \in N} h_{n,l} \cdot \{p_n + w_n - d_n\} \quad (17)$$

where

$$h_{n,l} = \zeta_{n,l} \cdot \pi^{(\circ)} + \sum_{k \in L} (\zeta_{n,k} \cdot \beta_{k,l} + \zeta_{n,l}) \cdot \pi^{(k)} \quad (18)$$

where $\pi^{(\circ)}$ is the probability of normal operation and $\pi^{(k)}$ is the probability of outage of line k . Then, by replacing $\zeta_{n,l}$ with $h_{n,l}$ in (7) and (16), the LTMs by considering credible $N - 1$ line-outage contingencies can be characterized accordingly.

In this study, $N - k$ contingencies are not considered, due to their very low probability of occurrence, as compared to $N - 1$ contingencies. Further, generator outage $N - 1$ contingencies are not considered either, since it is a nontrivial task to anticipate a redispatch rule for all generator outage cases in day-ahead schedules.

In real-time operations, wind power might be curtailed for the sake of system-wise reliability or prevention of congestion. Let \hat{w}_n and \hat{p}_l denote the nodal wind power and line flows with possible curtailment, respectively. Since $\hat{w}_n \leq w_n$, thus $\sigma_{\hat{w}_n} \leq \sigma_{w_n}$ holds as well. In addition, since the output power of wind farms within the same zone typically have positive correlations (i.e., \mathbf{R} is a non-negative matrix), then, it follows from (7) that the variance of \hat{p}_l would be no greater than that of p_l . Further, the first term in (16) would also become smaller for the cases of nodal curtailed wind power. Therefore, the LTM obtained from

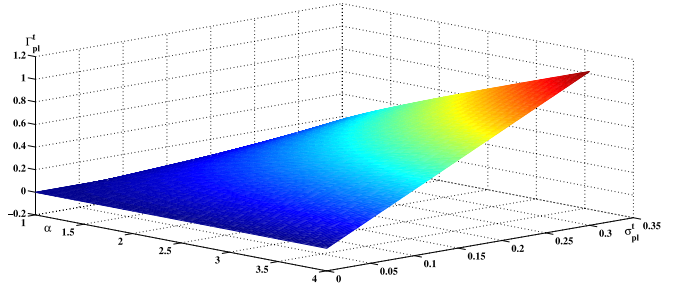


Fig. 1. Variations of Γ_l^t with respect to $\sigma_{p_l}^t$ and α .

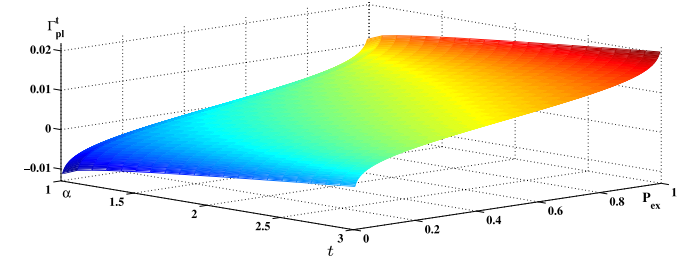


Fig. 2. Variations of Γ_l^t with respect to P_{ex} and α .

(16) also suffices to bound the congestion probability in (2) from above by $\frac{1}{\alpha^2}$ for the cases of curtailed nodal wind power.

C. Sensitivity of LTM Parameters

Eq. (16) characterizes LTMs, which establishes the relationship between the wind power forecast, w_n^t , the operator conservativeness on line congestion, α , and the variation of branch flows due to the wind power uncertainty, $\sigma_{p_l}^t$. Here, a study is performed on IEEE RTS96 system [28] with eight wind farms located at buses 3, 5, 10, 11, 16, 17, 19 and 22. For the day-ahead point forecast of wind power, 80% probability of exceedance is adopted ($P_{ex} = 0.8$). This indicates that the actual wind power will be more than the forecasted value with the likelihood of at least 80%. The point forecast approach is still widely-used by electric utilities, such as ERCOT, for day-ahead UC applications [29].

Fig. (1) depicts the variations of Γ for a branch with respect to changes in σ_{p_l} and α values. As can be seen, the value of Γ increases when α is higher, representing more conservative decision on transmission security by the operator and a larger LTM, and indeed, a larger transmission reserve. Γ increases also monotonically when σ_{p_l} is higher, reflecting the impact of wind power forecast uncertainty on the LTM. In other words, equations (9)–(16) denote that when the wind power forecast accuracy is shakier, as expressed by σ_w , the LTM variance, σ_{p_l} , will thereby increase, and thus, larger LTM values will be ensued.

The operator's assurance in the wind power forecast is inherent in the value that operator assigns to P_{ex} . The lower P_{ex} conveys that a larger value from wind power forecast distribution is determined as the point forecast, an indication of a more reliable forecast. Fig. 2 demonstrates the variations of Γ with respect to P_{ex} and α . In this figure, the value of σ_w is assumed to be 10% of the mean value. It can be observed that Γ rises with

P_{ex} . On the other end, Γ can be rarely negative when the assurance in the wind power forecast is high by choosing small P_{ex} (or by considering larger wind power at w_n^t than its expected value, $E[w_n^t]$, i.e., on the right tail of the PDF). Another possible cause of negative Γ is taking high risks as to the selection of small α values, when the wind power flows are in the opposite direction of the dominant power flow of the line. Consequently, negative LTM for a line is an indication of no congestion risk for that line and will not be integrated in the risk-aware UC.

III. RISK-AWARE UNIT COMMITMENT WITH LTM

The UC problem determines the day-ahead operation status of thermal generation units, including the unit on/off status and the amount of power generation at minimum cost, while the unit and system constraints including LTM-based transmission constraint is satisfied. The objective is to minimize the total expected cost, which consists of the variable operation cost and spinning reserve cost, as well as the fixed costs including no-load cost and start-up cost.

$$\text{Min} : \sum_{t \in T} \sum_{g \in G} [c_g p_g^t + s c_g s u_g^t + n c_g u_g^t + r c_g r_g^t] \quad (19)$$

The constraints of this mixed-integer linear optimization problem are as follows.

A. The Unit Constraints

$$s u_g^t = u_g^t - u_g^{t-1} \quad (20)$$

$$u_g^t \in \{0, 1\}, s u_g^t \geq 0, t \in \mathcal{T}, g \in \mathcal{G} \quad (21)$$

$$u_g^t p_g^{\min} \leq p_g^t \leq u_g^t p_g^{\max} - r_g^t, t \in \mathcal{T}, g \in \mathcal{G} \quad (22)$$

$$p_g^t - p_g^{t-1} \leq R_g^U \quad (23)$$

$$p_g^{t-1} - p_g^t \leq R_g^D, t \in \mathcal{T}, g \in \mathcal{G} \quad (24)$$

$$r_g^t \leq R_g^{10} u_g^t, t \in \mathcal{T}, g \in \mathcal{G} \quad (25)$$

$$\sum_{s=t-UT_g+1}^t s u_g^s \leq u_g^t \quad (26)$$

$$\sum_{s=t-DT_g+1}^t s d_g^s \leq 1 - u_g^t \quad (27)$$

$$s u_g^t - s d_g^t = u_g^t - u_g^{t-1}, s d_g^t \geq 0, t \in \mathcal{T}, g \in \mathcal{G} \quad (28)$$

B. The System Constraints

$$\sum_{g \in \mathcal{G}} p_g^t = \sum_{n \in \mathcal{N}} [d_n^t - \hat{w}_n^t], t \in \mathcal{T} \quad (29)$$

$$\sum_{g \in \mathcal{G}} r_g^t \geq \sum_{n \in \mathcal{N}} [\gamma_d d_n^t + \gamma_w \hat{w}_n^t], t \in \mathcal{T} \quad (30)$$

$$\begin{aligned} p_l^t &= B_l \cdot \Delta \theta_l, l \in \mathcal{L} - P_l^{\max} + \Gamma_l^t \leq p_l^t \leq P_l^{\max} \\ &- \Gamma_l^t, t \in \mathcal{T}, l \in \mathcal{L} \end{aligned} \quad (31)$$

Eqs. (20)–(25) represent the conventional unit constraints. The modeling of the units on/off binary variable and the start-up variable is presented by (20)–(21). Eq. (22) identifies the maximum and minimum operating capacity of the generators. The maximum generation is capped to the maximum capacity minus the spinning reserve offered by the unit. Eq. (23) enforces the hourly ramp up/down rate constraints. Constraint (24) confines the reserve requirement to the 10-min power ramping capability. Constraints in Eq. (25) are the minimum up and down time constraints of generators.

Eqs. (26)–(28) are the system constraints. Constraint (26) is the nodal power balance constraint, which ensures that the net injection into a node equals the net withdrawal from the same. Eq. (27) establishes the minimum system-wide reserve requirement. Constraint (28) uses the DC power flow method to impose the transmission line ratings on the power flows without considering transmission losses. As observed, the LTMs are integrated into this constraint by subtracting Γ_l^t from the thermal limit P_l^{\max} .

IV. PERFORMANCE ASSESSMENT IN REAL-TIME DISPATCH

The scheduling framework adopted in this study is based on the typical two-stage market environment, i.e., the day-head and the real-time dispatch markets. The real-time dispatch determines the final production level of the online generators at minimum operation cost, satisfying the unit and system constraints.

$$\text{Min} : f(x) = \sum_{\rho=\rho_0}^{\rho_0+n_T} \left[\sum_{g \in \mathcal{G}} \frac{1}{n_T} (c_g p_g^\rho) u_g^{\left[\frac{\rho}{n_T}\right]+1} \right] \quad (32)$$

Subject to:

$$\sum_{g \in \mathcal{G}} p_g^\rho = \sum_{n \in \mathcal{N}} (d_n^\rho - w_{rt,n}^\rho) \quad (33)$$

$$u_g^{\left[\frac{\rho}{n_T}\right]+1} p_g^{\min} \leq p_g^\rho \leq u_g^{\left[\frac{\rho}{n_T}\right]+1} p_g^{\max}, \\ g \in \mathcal{G}, \rho \in \{\rho_0, \dots, \rho_0 + n_T\} \quad (34)$$

$$p_g^\rho - p_g^{\rho-1} \leq \frac{R_g^U}{n_T} \quad (35)$$

$$p_g^{\rho-1} - p_g^\rho \leq \frac{R_g^D}{n_T}, g \in \mathcal{G}, \rho \in \{\rho_0, \dots, \rho_0 + n_T\} \quad (36)$$

$$p_l^\rho = B_l \cdot \Delta \theta_l^{\rho}, -P_l^{\max} \leq p_l^\rho \leq P_l^{\max}, \\ l \in \mathcal{L}, \rho \in \{\rho_0, \dots, \rho_0 + n_T\} \quad (37)$$

Eq. (29) is the objective function of the real-time dispatch optimization. $u_g^{\left[\frac{\rho}{n_T}\right]+1}$ denotes the commitment of generator g in the SCUC time step corresponding to the real-time dispatch time slot ρ . In this study, the SCUC is solved on an hourly time step basis and the real-time dispatch is run based on 5-min time slots. Thus, the value of n_T is 12. Eq. (30) holds the nodal demand balance constraint. Eq. (31) limits the generator

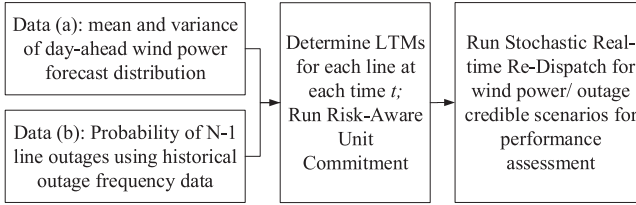


Fig. 3. Flowchart of conducting Risk-Aware UC with LTM method followed by ED.

dispatch variable to its maximum and minimum capacity. The ramp up/down rates are limited to their maximum cap scaled to the real-time dispatch time slot index ρ according to Eq. (32). The transmission capacity constraint is represented by Eq. (33). It is clear that unlike the day-ahead SCUC, the actual transmission ratings are enforced in the real-time operation. The conventional real-time dispatch is conducted on each time slot separately (e.g. every 5 to 15 min). Here, the real-time dispatch period is expanded to n_T time slots and the inter-temporal unit constraints are included to adapt the optimal dispatch results to the pragmatic ramping constraints. These constraints are crucial as they pose direct limits on the feasible activation of spinning reserves.

The main purpose of conducting the real-time dispatch process in this work is to examine the efficiency of the proposed method in reducing the security violations under real-time operation of power system (See Fig. 3). Therefore, the real-time dispatch model herein should be inclusively capable of identification of infeasible cases incurred by the constraint violations, such as transmission congestion, in advance and provide corrective measures to treat them. In this way, the performance of the proposed method in alleviating transmission congestion and increasing deliverable reserves will be examined in a systematic manner. In general, it is always possible that a feasible dispatch plan, wherein all security constraints are satisfied, does not exist due to the uncertainty of the renewable resources and potential contingencies. The procedures used to conduct corrective measures are described in the following.

A. Corrective Measures

Several remedies can be used by the power system operator to recover the economic dispatch from infeasibility, including wind power curtailment, using spinning reserve or activating nonspinning reserve, load shedding or demand response, fast-ramping units, as well as transmission reconfiguration. Implementing each corrective measure in the optimization problem can be generally represented by incorporating appropriate set of decision variables and their underlying constraints. Since the operator is willing to find a feasible solution in the corrective stage with minimal recovery costs, the least modification to the original operating condition is sought. Hence, the decision variables determining the corrective measures are accompanied by large penalty cost terms in the objective function. The choice of the penalty terms indicates the sensitivity of the factors contributing to the infeasibility which can be prioritized by the operator. For instance, the load and wind curtailment will be

penalized proportionate to the Value of Lost Load (VoLL), W_{ls} , and Value of Curtained Wind Power (VoCW), W_{cr} , respectively.

$$\text{Min : } f(\mathbf{X}) + h(\mathbf{Y}) \quad (34)$$

Subject to:

$$\mathbf{AX} + \mathbf{CY} \leq \mathbf{B} + \mathbf{D} \quad (35)$$

where $f(\mathbf{X})$ is the objective function of the original problem with \mathbf{X} as the original decision variables, and $h(\mathbf{Y})$ is the penalty cost term of the set of corrective decision variables \mathbf{Y} . \mathbf{A} and \mathbf{B} are the corresponding coefficients of the variables in the constraints and \mathbf{D} and \mathbf{B} are the right-side bounds. As an instance, for wind power curtailment and load shedding as two types of corrective measures, the term $h(\mathbf{Y})$ in the objective function can be specified by:

$$h(\mathbf{Y}) = \sum_{n \in N} \left(W_{cr} w_{cr,n}^\rho + W_{ls} p_{ls,n}^\rho \right) \quad (36)$$

The modified constraints in equation set (35) can be represented as:

$$\sum_{g \in \mathcal{G}} p_g^\rho = \sum_{n \in N} \left(d_n^\rho - w_{rt,n}^\rho - p_{ls,n}^\rho + w_{cr,n}^\rho \right) \quad (37)$$

$$w_{cr,n}^\rho \leq w_{rt,n}^\rho$$

$$p_{ls,n}^\rho \leq d_n^\rho$$

$$p_{ls,n}^\rho \geq 0$$

$$w_{cr,n}^\rho \geq 0, n \in \mathcal{N}, \rho \in \{\rho_0, \dots, \rho_0 + n_T\} \quad (38)$$

where $w_{cr,n}$ and $p_{ls,n}$ are the curtailed wind power and the load shedding, respectively.

Eq. (30) is modified as (37). Other constraints in (31)–(33) are still in place without any changes.

V. NUMERICAL RESULTS

The day-ahead UC and RTD model introduced in the previous sections are implemented in MATLAB and CPLEX and applied to the IEEE RTS96 [28]. Under normal operation, the UC results bring about the average utilization of branch capacities up to only 45% of the total line capacity. Therefore, in order to observe a considerable number of congestion cases in the case studies and examine the effectiveness of the proposed method on mitigation of congestion, the branch capacities are modified to the 45% of their nominal ratings. The load data and other characteristics of the system are kept unchanged. The real-time dispatch scheduling horizon is considered as one hour with $n_T = 12$ and the time slot of 5 mins.

The value of γ_d and γ_w for the reserve requirement in the UC are set to 3% and 5%, respectively. The penalized value of loss of load (VOLL) is considered to be 2,500 \$/MWh [30]. The wind power spillage cost is not considered in this study.

The wind power data is obtained from the West Texas Mesonet database [31] for 8 buses in ERCOT grid, and the wind farms are located at the same buses as in section II-C. The nominal generation capacity for all of the wind farms are scaled equally at 100 MW for the base scenario. In the case studies of this paper,

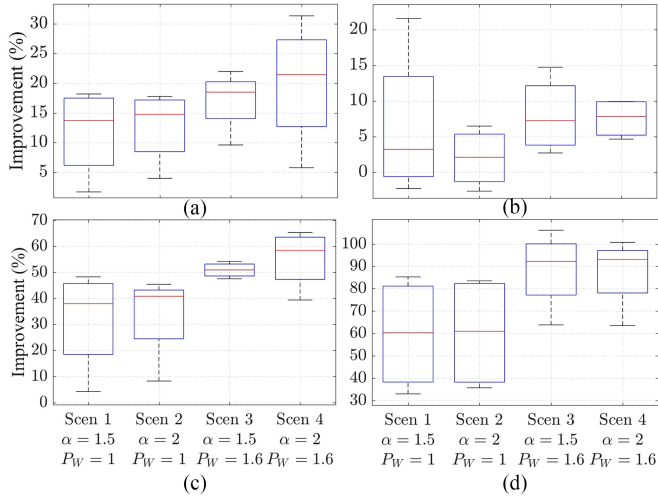


Fig. 4. Comparative results of real-time operation performance for four scenarios in terms of (a) percentage savings in the real-time operation costs; (b) percentage mitigation of real-time wind power curtailment; (c) percentage decrease in the real-time load shedding; and (d) percentage improvement in the real-time available spinning reserve capacity.

nodal wind power forecast is assumed to follow a truncated normal distribution within 0 to the corresponding rated capacity [32]. This is because multivariate normal probability distribution is fully characterized by its mean and covariance matrix. Using the correlation coefficient matrix R_w and the respective mean and variance of nodal wind power enables us to know the joint distribution and thus generate correlated wind power samples as test cases. The values of P_{ex} is chosen as 0.8.

$$w_n^t = E[w_n^t] - Q(P_{ex})\sigma_{w_n^t} \quad (39)$$

where $Q(\cdot)$ is the tail probability of the standard normal distribution. The standard deviation of forecast error is assigned as 10% of the mean (i.e. $\frac{\sigma_{\hat{w}_n}}{\mu_{\hat{w}_n}} = 0.1$).

In order to incorporate various input load and wind power conditions, a comprehensive study is performed by simulating the day-ahead UC and RTD for the input data of the total 365 days of a year. The study is carried out for four different scenarios with respect to the wind power level P_W and the α value (Scen. 1: $P_W = 1$, $\alpha = 1.5$; Scen. 2: $P_W = 1$, $\alpha = 2$; Scen. 3: $P_W = 1.6$, $\alpha = 1.5$; and Scen. 4: $P_W = 1.6$, $\alpha = 2$). The unity value for the wind level corresponds to the original wind power data and value of 1.6 implicates that the wind power input is boosted to 1.6 times of the original data. In this way, the robustness of the proposed method in system operations under extremely high wind power scenarios is estimated. The obtained real-time dispatch results by using the proposed UC framework with LTMs are compared with the same using the conventional UC formulation.

In Fig. (4), the distribution of percentage change of the operational outcomes with LTM are plotted to demonstrate the effectiveness of the proposed method by comparing it to the conventional method. Considering the latter as reference, the changes are calculated as follows:

$$\text{Change (\%)} = \frac{\Delta y^{\text{Conv., PM}}}{y^{\text{Conv.}}} \times 100 \quad (40)$$

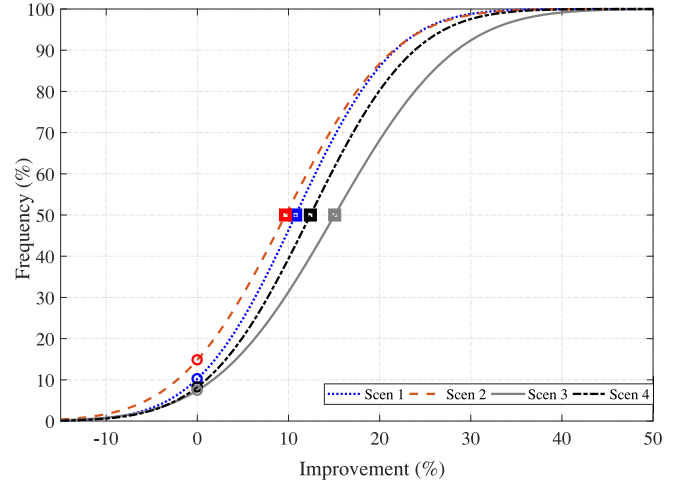


Fig. 5. CFF of improvements in alleviating transmission congestion by adopting preventive LTM.

For the operation cost, wind power curtailment and load shedding, $\Delta y^{\text{Conv., PM}}$ equals the value for conventional method minus that for PM, and vice versa for the available reserve. Each box depicts the low, median, high and 25th and 75th percentile for each of the four case study scenarios given the 365 days of input data during a year. The wind power level and α value for each scenario corresponding to each boxplot is indicated under the horizontal axis. The subplots in Fig. 4 are as follows. Part (a) is the percentage savings in the real-time operation costs. For scenarios 3 and 4, where the wind power level is more significant compared to scenarios 1 and 2, the proposed method demonstrates larger impact on reduction of operation costs. Specifically, in scenario 4, the high tail is 33% whereas in scenario 2 it is 17%. It can be also inferred that the scenarios with larger α present superior results. Part (b) is the percentage mitigation of real-time wind power curtailment. It is observed that in scenario 1, the wind high tail and 75% value are the highest among 4 scenarios, but the median value is lower than scenarios 3 and 4 with larger wind level. Thus, the impact of the proposed method on wind power curtailment is more pronounced when the wind power level is larger. Part (c) depicts the the percentage decrease in the real-time load shedding, as well as part (d) is the percentage improvement in the real-time available spinning reserve capacity, wherein more improvement is evident in scenarios 3 and 4 with larger wind power level. In overall, it is observed from all parts of Fig. 4 that the proposed method delivers positive improvements for all the scenarios.

Fig. (5) represents the improvements in transmission congestion alleviation in the form of a cumulative frequency function (CFF) of congested hours. A normal distribution function is fitted to the data. This figure conveys the likelihood of success in decreasing the congestion events. The point corresponding to the mean value and the point corresponding to zero improvements are pinpointed by markers. As can be seen, the odds of having zero improvement or below is only 15% in scenario 1 and less than 10% in scenarios 2, 3 and 4. Moreover, for an odds of 50% ratio of the total observed points, the percentage reduction in the congestion events in this system is around 10% for scenarios 1

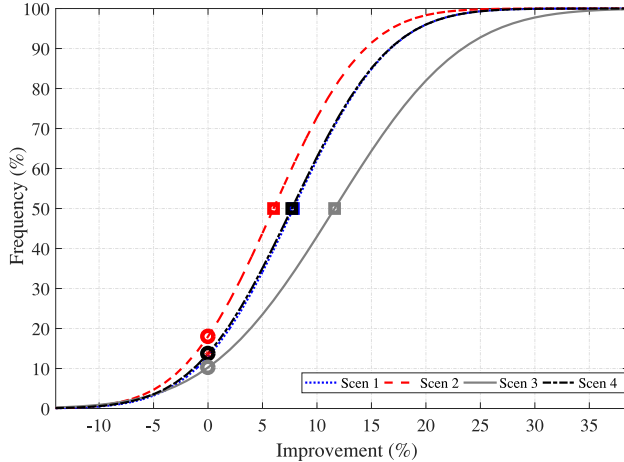


Fig. 6. CDF of improvements in reduction of the need to corrective measures in RTD due to infeasibilities in real-time dispatch by adopting preventive LTM.

and 2. For scenarios 3 and 4, this value is 16% and 13%, respectively. This result implies that the effectiveness of the proposed method in congestion alleviation is more remarkable in case of larger wind power.

From the aforementioned results in scenarios 3 and 4, it can be further observed that the proposed method is robust to the extreme wind power generations, conveying that the 60% increase in the wind power generation level has not jeopardized the quality of the proposed method in congestion mitigation.

In Fig. (6), the performance improvements in terms of reduction of the need to corrective measures in RTD due to infeasibilities by adopting the proposed method is depicted in the form of CFF. This figure indicates the impact of the proposed method to provide a larger feasible region by better utilization of the available resources. It remarks that the proposed method not only achieves more effective elimination of transmission congestion, but also can mitigate any infeasibilities with respect to violation of the constraints.

Wind power curtailment generally contradicts the operation cost and transmission congestion. For instance, the wind power curtailment can be a remedy for mitigation of transmission congestion. For a range of wind power levels between 1 and 1.6, Figs. (7) and (8) depict the total real-time operation cost and the congestion hours versus the wind power curtailment, respectively. The dash-dot black curve corresponds to the conventional UC whereas the other three curves correspond to the proposed method (denoted by PM) with three different α values. It can be seen that these three curves are well below the black one, denoting reduction in operation cost and congestion events with different α and wind power levels and confirming robust performance of the proposed method. Note that assigning a larger α value would reduce the congestion events but may increase the total cost compared to smaller α values (See the red curve in Fig. (7)). Further, Fig. (7) shows that regardless of using the LTMs, the increase to a certain level of wind power generation ($P_W = 1.2$) decreases the operation cost, however, for higher wind power levels, the system operation cost starts raising.

In the light of these observations, it is concluded that the proposed method can reduce redispatch costs, alleviate wind power

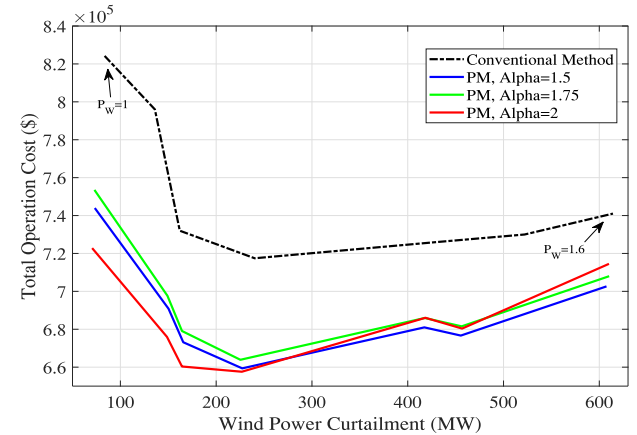


Fig. 7. Total operation cost versus wind power curtailment.

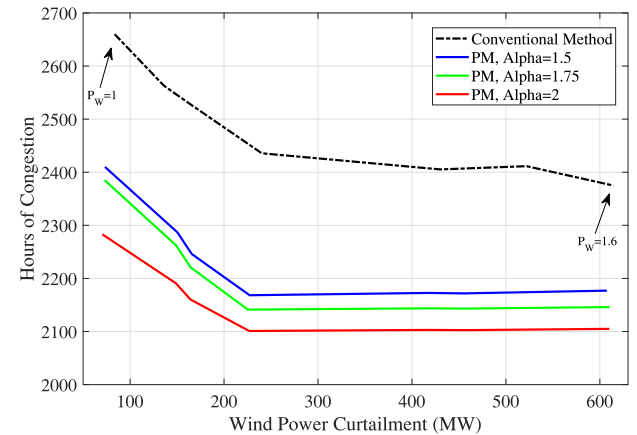


Fig. 8. Total congestion hours versus the wind power curtailment.

curtailment and load shedding events, improve the system robustness to transmission congestion, and enhance the operation reliability by means of available reserve capacity.

VI. CONCLUSION

Although wind generation is generally considered an energy source with zero marginal cost, it can impose operational costs due to lack of dispatchability and the forecast errors in wind resource availability. In this paper, a risk-aware UC approach is proposed with the aim to reach a cost-effective real-time dispatch while improving the wind power utilization as well as alleviation of transmission congestion. Using the proposed LTM, the impact of multi-locational wind power uncertainty and correlation on the transmission capacity constraint in the UC problem is quantified. Thus, the proposed method can reduce wind integration and forecast error costs, as the day-ahead committed units and reserve resources are more diverse and power flow dispatch can fittingly follow the information regarding the uncertainty in wind power forecast by using LTM signals. Demonstrated results and analysis confirm that using this approach outperforms the conventional UC and RTD framework to enhance the reliability of power system operations with wind

power integration, while leading to more cost-effective power system operation.

ACKNOWLEDGMENT

The authors would like to thank Dr. K. Hedman from Arizona State University for his valuable feedback on this work and also would like to thank to West Texas Mesonet Team for granting us access to their wind power measurement database, and to the anonymous reviewers for their constructive comments.

REFERENCES

- [1] L. Bird, J. Cochran, and X. Wang, "Wind and solar energy curtailment: Experience and practices in the united states," Nat. Renewable Energy Lab., Denver, CO, USA, Tech. Rep. NREL/TP-6A20-60983, 2014.
- [2] B. Fox, *Wind Power Integration: Connection and System Operational Aspects*, Herts, U.K.: IET, 2007.
- [3] J. M. Morales, A. J. Conejo, and J. Pérez-Ruiz, "Economic valuation of reserves in power systems with high penetration of wind power," *IEEE Trans. Power Syst.*, vol. 24, no. 2, pp. 900–910, May 2009.
- [4] C. De Jonghe, B. F. Hobbs, and R. Belmans, "Value of price responsive load for wind integration in unit commitment," *IEEE Trans. Power Syst.*, vol. 29, no. 2, pp. 675–685, Mar. 2014.
- [5] L. Vargas, G. Bustos-Turu, and F. Larraín, "Wind power curtailment and energy storage in transmission congestion management considering power plants ramp rates," *IEEE Trans. Power Syst.*, vol. 30, no. 5, pp. 2498–2506, Sep. 2015.
- [6] A. Nasri, A. J. Conejo, S. J. Kazempour, and M. Ghandhari, "Minimizing wind power spillage using an OPF with facts devices," *IEEE Trans. Power Syst.*, vol. 29, no. 5, pp. 2150–2159, Sep. 2014.
- [7] F. B. Alhasawi and J. V. Milanovic, "Techno-economic contribution of facts devices to the operation of power systems with high level of wind power integration," *IEEE Trans. Power Syst.*, vol. 27, no. 3, pp. 1414–1421, Aug. 2012.
- [8] J. Matevosyan, M. Olsson, and L. Söder, "Hydropower planning coordinated with wind power in areas with congestion problems for trading on the spot and the regulating market," *Elect. Power Syst. Res.*, vol. 79, no. 1, pp. 39–48, 2009.
- [9] R. Jiang, J. Wang, and Y. Guan, "Robust unit commitment with wind power and pumped storage hydro," *IEEE Trans. Power Syst.*, vol. 27, no. 2, pp. 800–810, May 2012.
- [10] A. A. S. de la Nieta, J. Contreras, and J. P. S. Catalão, "Optimal single wind hydro-pump storage bidding in day-ahead markets including bilateral contracts," *IEEE Trans. Sustain. Energy*, vol. 7, no. 3, pp. 1284–1294, Jul. 2016.
- [11] R. Loisel, A. Mercier, C. Gatzen, N. Elms, and H. Petric, "Valuation framework for large scale electricity storage in a case with wind curtailment," *Energy Policy*, vol. 38, no. 11, pp. 7323–7337, 2010.
- [12] R. Sioshansi, "Evaluating the impacts of real-time pricing on the cost and value of wind generation," *IEEE Trans. Power Syst.*, vol. 25, no. 2, pp. 741–748, May 2010.
- [13] M. Matos and R. J. Bessa, "Setting the operating reserve using probabilistic wind power forecasts," *IEEE Trans. Power Syst.*, vol. 26, no. 2, pp. 594–603, May 2011.
- [14] L. Xie, Y. Gu, X. Zhu, and M. G. Genton, "Short-term spatio-temporal wind power forecast in robust look-ahead power system dispatch," *IEEE Trans. Smart Grid*, vol. 5, no. 1, pp. 511–520, Jan. 2014.
- [15] S. Abedi, G. H. Riahy, M. Farhadkhani, and S. H. Hosseiniyan, "Improved stochastic modeling: An essential tool for power system scheduling in the presence of uncertain renewables," in *New Developments in Renewable Energy*, Rijeka, Croatia: InTech, 2013, pp. 101–120.
- [16] C. Shao, X. Wang, M. Shahidehpour, X. Wang, and B. Wang, "Security-constrained unit commitment with flexible uncertainty set for variable wind power," *IEEE Trans. Sustain. Energy*, vol. 8, no. 3, pp. 1237–1246, Jul. 2017.
- [17] F. Wang and K. W. Hedman, "Dynamic reserve zones for day-ahead unit commitment with renewable resources," *IEEE Trans. Power Syst.*, vol. 30, no. 2, pp. 612–620, Mar. 2015.
- [18] S. Abedi, M. He, and M. Giessmann, "Graph partitioning-based zonal reserve allocation for congestion management in power systems with wind resources," in *Proc. IEEE North Amer. Power Symp.*, 2016, pp. 1–6.
- [19] K. W. Hedman, R. P. O'Neill, E. B. Fisher, and S. S. Oren, "Optimal transmission switching with contingency analysis," *IEEE Trans. Power Syst.*, vol. 24, no. 3, pp. 1577–1586, Aug. 2009.
- [20] F. Qiu and J. Wang, "Chance-constrained transmission switching with guaranteed wind power utilization," *IEEE Trans. Power Syst.*, vol. 30, no. 3, pp. 1270–1278, May 2015.
- [21] L. Roald, F. Oldewurtel, T. Krause, and G. Andersson, "Analytical reformulation of security constrained optimal power flow with probabilistic constraints," in *Proc. IEEE Grenoble Conf.*, 2013, pp. 1–6.
- [22] M. Nick, O. Alizadeh-Mousavi, R. Cherkaoui, and M. Paolone, "Security constrained unit commitment with dynamic thermal line rating," *IEEE Trans. Power Syst.*, vol. 31, no. 3, pp. 2014–2025, May 2016.
- [23] B. Banerjee, D. Jayaweera, and S. Islam, "Impact of wind forecasting and probabilistic line rating on reserve requirement," in *Proc. IEEE Int. Conf. Power Syst. Technol.*, 2012, pp. 1–6.
- [24] L. Wu, M. Shahidehpour, and Z. Li, "Comparison of scenario-based and interval optimization approaches to stochastic SCUC," *IEEE Trans. Power Syst.*, vol. 27, no. 2, pp. 913–921, May 2012.
- [25] M. He, S. Abedi, and A. Boker, "Line transfer margin-based congestion management with multi-correlated wind power," in *Proc. IEEE, Power Energy Soc. Gen. Meeting*, 2015, pp. 1–5.
- [26] D. P. Dubhashi and A. Panconesi, *Concentration of Measure for the Analysis of Randomized Algorithms*. Cambridge, U.K.: Cambridge Univ. Press, 2009.
- [27] L. Min and P. Zhang, "A probabilistic load flow with consideration of network topology uncertainties," in *Proc. IEEE Int. Conf. Intell. Syst. Appl. Power Syst.*, 2007, pp. 1–5.
- [28] P. Wong *et al.*, "The IEEE reliability test system-1996. a report prepared by the reliability test system task force of the application of probability methods subcommittee," *IEEE Trans. Power Syst.*, vol. 14, no. 3, pp. 1010–1020, Aug. 1999.
- [29] "ERCOT nodal Protocols," Elect. Rel. Council Texas, Austin, TX, 2013.
- [30] J. M. Chamorro, L. M. Abadie, and R. de Neufville, "Measuring performance of long-term power generating portfolios," in *Green Energy and Efficiency*. Berlin, Germany: Springer, 2015, pp. 395–428.
- [31] "West Texas Mm," 2015. [Online]. Available: <http://www.mesonet.ttu.edu/>
- [32] A. Lau and P. McSharry, "Approaches for multi-step density forecasts with application to aggregated wind power," *Ann. Appl. Stat.*, vol. 4, pp. 1311–1341, 2010.

Sajjad Abedi (S'9–M'17) received the B.Sc. and M.Sc. degrees (with hon.) in electrical engineering from the Isfahan University of Technology, Isfahan, Iran and the Amirkabir University of Technology (Tehran Polytechnic), Tehran, Iran, respectively, and the Ph.D. degree in electrical engineering from Texas Tech University, TX, USA, in 2017.

He is currently a Postdoctoral Research Fellow with the School of Mechanical Engineering and Department of Mathematics, Purdue University, IN, USA. His research interests include power system modeling and operations, renewable energy integration, uncertainty and risk modeling, and predictive data analytics.

Miao He (M'13–SM'17) received the B.S. degree from the Nanjing University of Posts and Telecommunications, Nanjing, China, in 2005; the M.S. degree from Tsinghua University, Beijing, China, in 2008; and the Ph.D. degree from Arizona State University, Tempe, AZ, USA, in 2013.

He is currently an Assistant Professor with Texas Tech University, Lubbock, TX, USA. His current research interests include stochastic modeling and data analytics for smart grids, wind power systems, and cyber-physical systems.

Diran Obadina (SM'17) received the B.Sc. degree from the University of Ife, Ife, Nigeria, the M.Sc.E. degree from the University of New Brunswick, Fredericton, NB, Canada, and the Ph.D. degree from the University of Calgary, Calgary, AB, Canada all in electrical engineering. He is a Principal Engineer with the Electric Reliability Council of Texas (ERCOT), Taylor, TX, USA, with responsibility for strategic development of applications and systems needed for reliability and energy markets operations. Before joining ERCOT in 2003 as a Manager of Development of Energy and Market Management Systems, he was a Senior Staff Engineer with Siemens Energy and Automation, involved with the development and delivery of Energy Management Systems and Market Management Systems. His professional interests are in the areas of power systems modeling, power systems analytical methods, power systems optimization, and renewable integration.